Journal of
Composites Science

MDPI

Article

Effect of Doping on Phase Formation in YBCO Composites

Sanat Tolendiuly [1,*], Aigerim Sovet [1,2] and Sergey Fomenko [2]

[1] Space Engineering Department, Almaty University of Power Engineering and Telecommunications Named After Gumarbek Daukeyev, Almaty 050013, Kazakhstan; a.sovet@aues.kz
[2] Laboratory of SHS–New Materials, Institute of Combustion Problems, Almaty 050012, Kazakhstan; exotherm@yandex.kz
* Correspondence: s.tolendiuly@aues.kz

Abstract: This article discusses an effective method for obtaining superconducting composites based on $Y_1Ba_2Cu_3O_{7-\delta}$ (YBCO) by optimizing the total preparation time in comparison with similar scientific works while searching for effective modifying micro-additives. YBCO-based composites were doped with microparticles of aluminum, nickel, and iron. It was established that the initial ratio of green components, heat treatment, and holding time directly affect the qualitative and quantitative formation of the useful superconducting phase Y_{123}, which in turn affects the basic superconducting properties of the final material.

Keywords: high-temperature superconductors; composites; doping; combustion; microparticles

Citation: Tolendiuly, S.; Sovet, A.; Fomenko, S. Effect of Doping on Phase Formation in YBCO Composites. *J. Compos. Sci.* **2023**, *7*, 517. https://doi.org/10.3390/jcs7120517

Academic Editors: Francesco Tornabene and Jinyang Xu

Received: 16 October 2023
Revised: 7 December 2023
Accepted: 13 December 2023
Published: 15 December 2023

1. Introduction

Cuprate-based high-temperature superconductors (HTSCs) have attracted much attention from researchers and engineers due to their unique properties and potential for various practical applications. Superconductivity is the effect of zero electrical resistivity in a material at a temperature below the critical temperature Tc. This means that the electric current, once generated, continues to flow without the consumption of external energy and without any losses. Along with zero resistivity, the Meissner effect occurs when the magnetic field around the superconductor does not change, which most often manifests itself in the levitation of superconducting materials above magnets (or vice versa). In addition, superconductors are ideal diamagnets at temperatures above absolute zero [1–3]. The main characteristic of superconductors is the critical temperature (Tc) which is the temperature at which a material transitions from the normal (usually dielectric) state to the superconducting state.

In studies of cuprate-based superconducting materials, doping plays an important role. Doping is the process of introducing certain useful impurities into the composition of a material (metal, alloy, semiconductor). Doping is used to change or improve the physical and chemical properties of the final materials. Doping can affect the oxidation state of copper in Cu-O layers, which has significant implications for the superconducting properties of cuprate materials.

In the article "Study of $Y_1Ba_2Cu_3O_{7-\delta}$ + CuO Nanocomposite as a Resistive Current Limiter" [4], the authors studied the effect of nanosized CuO inclusions as the second component of composites on the transport properties of superconducting polycrystals $YBa_2Cu_3O_7$. $YBa_2Cu_3O_{7-\delta}$ samples with different contents of CuO nanoparticles were synthesized. The magnetic properties were analyzed within the framework of the extended critical state model. It was established that the addition of 20 wt% CuO nanoparticles leads to an increase in the critical current density at T = 77 K. This increase in the critical current can be explained by the presence of CuO nanoparticles that appear on the surface of superconducting materials. These samples become effective anchoring centers for Abrikosov vortices. The paper presents the results of experimental studies of a switching

superconducting short-circuit current limiter in alternating voltage networks based on second-generation superconductors (HTSC). The test equipment contains a series connected HTSC module and a high-speed current switch with a tripping time of 9 ms. The high efficiency of samples made of the $Y_1Ba_2Cu_3O_{7-\delta}$ + CuO nanocomposite material as an active element of a resistive current limiter was demonstrated. In the article, the mixture was pressed into a cylindrical mold with a diameter of 10 mm and a length of 50 mm under a pressure of 10 MPa. The samples were then sintered at 940 °C for 24 h, followed by cooling to room temperature in an air oven.

In another scientific work [5], the influence of magnetic impurities Fe, Co, and Ni on the superconductivity of the cuprate superconductor $Y_1Ba_2Cu_3O_{7-\delta}$ (Y_{123}) was studied to study the behavior of Tc. A solid-phase synthesis method was used to obtain fully oxygenated $Y_{1-x}M_xBa_2Cu_3O_{7-\delta}$ (Y1-xMx-123) samples with low doping levels ($0.00000 \leq x \leq 0.03000$). In this work, the samples were thoroughly mixed, crushed, and calcined in air at 850 °C for 24 h in an alumina crucible. Calcination was repeated twice with intermediate grinding. To obtain samples completely saturated with oxygen, the samples were annealed in a flow of oxygen for 24 h at a temperature of 930 °C, followed by slow cooling over 10 h to room temperature. The article pays more attention to the sample processing stage; AC magnetic susceptibility measurement results for the Y1-xMx-123 series (M = Co, Fe, Ni). It was found that Tc initially increased with the addition of magnetic impurities to the optimum content, $x \approx 0.01$, 0.004, 0.004 for Co, Fe, and Ni dopants, respectively. While the pure sample had Tc = 90.91 K, it was observed that Co(Fe) impurity amounting to almost 1% (0.4%) increased it to 92.75 K. Ni substitution also showed the same trend. Tc peaks at the optimum Co doping level were seen before decreasing due to overdoping. Similar trends were found for samples doped with Fe and Ni. Interestingly, the increase in Tc with magnetic replacements contradicts the Abrikosov–Gorkov theory, which predicted a decrease in Tc. Moreover, the addition of Fe (0.4%) and Co (1%) resulted in an equal increase in Tc. Comparing a sample doped with almost 0.4% Co with a sample doped with 0.4% Fe, we observed a higher Tc in the latter case of 0.8 K despite almost equal ionic radii, while Fe has a higher high intrinsic magnetic moment compared to Co. However, in compounds doped with Ca and Sr, no increase in Tc was found, which may indicate the effective role of magnetic atoms in increasing Tc.

In article [6], a study was carried out on $Y_1Ba_2Cu_3O_{7-\delta}$ (YBCO) superconductors, in which $BaTiO_3$ and WO_3 particles were introduced as artificial pinning centers. These pinning centers play an important role in improving the superconducting properties of the material. First, the researchers analyzed the phase purity of the material using X-ray diffraction. Then, they showed that the incorporation of $BaTiO_3$ and WO_3 particles not only did not disturb the phase purity of YBCO, but also led to the formation of isolated secondary phases enriched in tungsten (W). Scanning electron microscopy revealed that the $BaTiO_3$ and WO_3 particles tended to be located at grain boundaries, acting as bridges connecting the superconducting YBCO sample. This provides additional paths for magnetic flux and improves the superconducting properties of the material. Measurements of superconducting properties showed significant improvement. The H_{c2} (critical magnetic field) values increased from 1.6 T to 3.4 T after the addition of $BaTiO_3$ and WO_3. Also, superconductivity parameters improved, measured by alternating current susceptibility, indicating an increase in the critical current. This may make YBCO materials with artificial pinning centers more suitable for practical applications.

In a further paper [7], the influence of preforming sample pressure on the morphology and superconducting properties of bulk YBCO samples was studied. The mixture was pressed at various pressure values. The results showed that the sample preforming pressure plays an important role. Specimens compacted at 200 MPa exhibited high levitation force and trapped field properties, while specimens compacted at 300 MPa exhibited microdefects and lower performance. Thus, a pressure of 200 MPa is considered optimal for stable production of samples without macro-defects with high performance. Superconducting property measurements also showed that the preforming pressure affects superconducting

performance. Samples pressed at 200 MPa and 300 MPa had higher values of critical current and levitation force compared to samples pressed at 100 MPa.

In recent years, research was also carried out on $ReBa_2Cu_3O_{7-}x$ superconductors, where yttrium (Y) was replaced by rare earth elements. These studies focused on the electrical and structural properties of materials. The authors of the article [8] studied the structural properties of materials in which Gd, Sm, and Nd replaced Y in equal proportions. This made it possible to understand how substitutions of rare earth elements affect the structure of superconductors.

In our previous article "Properties of high-temperature superconductors (HTS) and synthesis technology" [9], the main results of research related to the synthesis and study of HTSC materials, namely cuprates obtained by combustion synthesis, were presented. In this article, a comprehensive study was carried out on the influence of various factors, namely, the ratio of the initial components, annealing temperature, and holding time on the formation of the superconducting Y_{123} phase in the composition of materials. The researchers found that the ratio of the starting components plays a key role in the formation of the superconducting phase. Optimal results were achieved at certain annealing temperatures and holding times. The qualitative and quantitative formation of the conducting phase was highly dependent on these parameters. The study also included an analysis of the chemical and phase composition of the obtained samples, as well as a study of their morphology. Optimal results were achieved under the following conditions: annealing temperature 920 °C and holding time for 10 h. These parameters made it possible to obtain the maximum amount of superconducting phase in the Y-Ba-Cu-O system. This result highlights the importance of fine-tuning the entire synthesis process to achieve the desired superconducting properties.

The physical properties of composite superconductors mainly depend on synthesis methods and technological aspects of the preparation of initial samples. Today, the main efforts of scientists from all over the world are aimed at reducing costs and time in obtaining superconducting materials with the desired properties. Synthesis routes for cuprate superconductors are aimed at improving the properties of these materials, such as obtaining pure phases, grain uniformity, better connectivity between grains, and high electric current density. Research into new methods for the synthesis of oxide superconductors is focused on obtaining materials with higher Tc and Jc [10]. Chemical methods such as sol-gel, furnace, co-precipitation and hydrothermal, as well as the use of microwaves have been used in the synthesis of superconducting materials due to the homogeneity in obtaining samples [10–13].

The YBCO superconductor is usually synthesized by solid phase reaction method. However, this method has some disadvantages due to the long sample preparation procedure and long synthesis time—about 50 h to 100 h for the procedure, which is usually repeated up to three times in a controlled oxygen atmosphere. As a result, there is a search for alternative methods for producing this superconductor to optimize the amount of material obtained or simplify procedures.

This work describes the synthesis of superconducting composites containing various metal microparticles and analyzes their effect on the formation of a useful superconducting phase (Y_{123}) and on the critical temperature Tc. In comparison with the above-mentioned scientific works of other scientists, it should be noted that we managed to reduce the obtained procedure by decreasing the holding time up to 10 h (almost 2.4 h less), thanks to the inclusion of a technological process, namely, preliminary mechanical activation of the initial green components (before the solid-phase combustion synthesis) which promote the maximum yield (formation) of the superconducting phase (Y_{123}) in the final material.

2. Materials and Methods

2.1. Synthesis

2.1.1. Initial Green Components

Y_2O_3 powder (purity 99%, 50–60 microns), BaO (purity 99%, 45–60 microns), nano-copper oxide (purity 99%, 30–50 nm), Al (purity 99%, 600–610 μm), Ni (purity 99.9%, 20–25 μm), Fe (purity 99.9%, 250–260 μm) were used as starting components to produce superconducting composites of YBCO.

2.1.2. Sample Preparation

The initial powders with a mass ratio of (Y:Ba:Cu:O) + X = (17%:46%:29%:8%) + X% (where X is the doping component) were weighed, thoroughly mixed, and ground in a porcelain mortar to obtain a homogeneous mixture over 10 min. The mixture was then cold pressed (80 MPa) into cylindrical specimens with a diameter of 2.0 cm and a height of 5 cm using a hydraulic press. These samples were then calcined in a muffle furnace (in a normal atmospheric environment) at 920 °C for 10 h. They were then fired at 920 °C (heating rate 100 °C/min) for 10 h under oxygen flow (278 mL/min). Presumably the chemical reaction proceeds by the following format:

$$Y_2O_3 + 4BaO + 6CuO + 1/2O_2 = 2YBa_2Cu_3O_{7-x}$$

The main purpose of calcination is the decomposition of precursors, which ensures the possibility of diffusion mixing of the latter, thereby contributing to the formation of an ideal stoichiometric superconducting phase $YBa_2Cu_3O_7$. It is worth noting that the orthorhombic superconducting phase Y_{123} is unstable at temperatures above 950 °C. Below 900 °C, two new superconducting phases appear as $YBa_2Cu_4O_8$ and $Y_2Ba_4Cu_7O_{14}$, and the main superconducting phase Y_{123} becomes unstable. It should be emphasized that in the temperature range from 900 °C to 950 °C, if the oxygen content per formula unit is less than 6.5, the structure of the material becomes tetragonal and the material loses superconducting properties, since the Y_2BaCuO_5 (Y_{211}) phase is formed. To restore the oxygen content to the desired value, close to seven by indices, the sample was annealed in a flow of oxygen O_2 at a temperature of 920 °C. This allows one to capture the required amount of oxygen and restore the necessary structure. The obtained sample color was black.

2.1.3. Preliminarily Mechanical Activation

Mechanical activation is the process of activating solids by mechanically treating them. This process includes not only grinding, but also the creation of structural defects, changes in surface curvature, phase transformations, and even amorphization of crystals. It is important to note that mechanical activation can occur without grinding, but grinding is always accompanied by activation.

For mechanical activation of the initial powders, a planetary ball mill was used (Figure 1). The original powders were placed in the machine in a 1:2 ratio with porcelain balls. Porcelain balls were used instead of steel balls to avoid unwanted reactions with the test powders. The rotation speed was 320 rpm, and the time of mechanical activation of the powders varied with the following parameters: 10, 20, 30, 40, and 50 min.

According to our research (Figure 2), we determined the optimal mechanical activation mode as 30 min. With 30 min of mechanical activation of the formation of the superconducting phase, Y_{123} was the highest compared to the others.

Figure 1. Planetary ball mill (Retsch PM 200F).

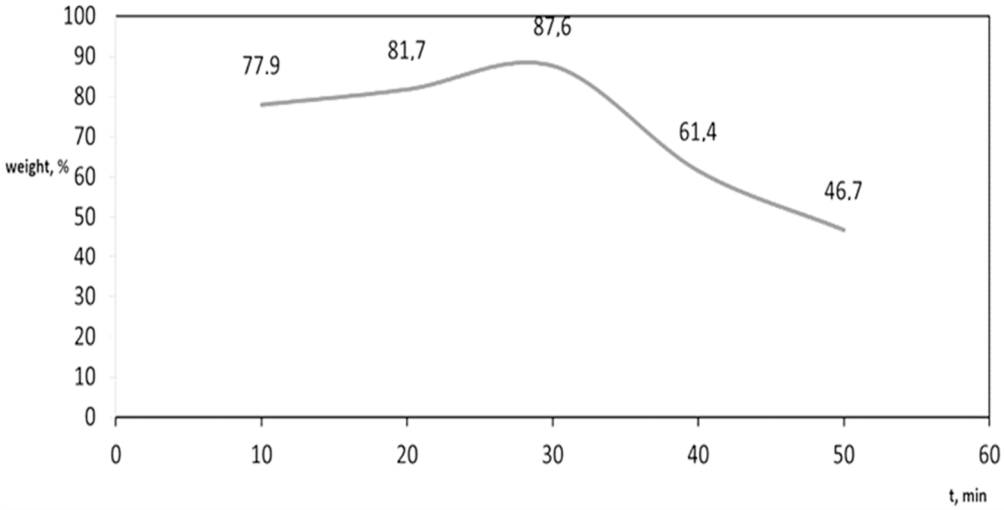

Figure 2. Dependence of the yield of the expected phase $YBa_2Cu_3O_{7-\delta}$ on the time of mechanical activation.

2.1.4. Chemical Doping

Superconducting samples containing microparticles of various metals were prepared with nominal stoichiometry (Table 1), where x = 0, 0.3, 0.5, 0.7, 1.0 is the percentage of doping with Al, Ni, Fe microparticles.

The selection of these doping components was briefly explained in the Introduction Section. Fe, Co, Ni, and Al atoms were chosen as the doping elements to identify the influence of magnetic and non-magnetic particles on phase formation and superconducting properties as well. The second reason for adding Al microparticles is that it has significant effects on the chemical reaction speed (diffusion) due to its good reactivity. $YBa_2Cu_3O_{7-\delta}$ (or Y_{123}) samples doped with microparticles are materials based on artificial superconductors with the formula $YBa_2Cu_3O_{7-\delta}$@X, into which modifying impurities are introduced to change their properties. Doping microparticles into the YBCO matrix can affect the electrical properties of the superconductor, such as the critical transition temperature to the superconducting state (T_c), magnetic properties, conductivity, and other parameters. These changes may result from the influence of the electronic structure and the interaction between the doping element atoms and YBCO.

Table 1. Composition of pure and doped samples.

Name	Doping Element
$YBa_2Cu_3O_{7-x}$ (Y_{123})	0%
$Y_{123}@Al_{0.1}$	Al (0.1%)
$Y_{123}@Al_{0.3}$	Al (0.3%)
$Y_{123}@Al_{0.5}$	Al (0.5%)
$Y_{123}@Al_{0.7}$	Al (0.7%)
$Y_{123}@Al_{1}$	Al (1%)
$Y_{123}@Ni_{0.1}$	Ni (0.1%)
$Y_{123}@Ni_{0.3}$	Ni (0.3%)
$Y_{123}@Ni_{0.5}$	Ni (0.5%)
$Y_{123}@Ni_{0.7}$	Ni (0.7%)
$Y_{123}@Ni_{1}$	Ni (1%)
$Y_{123}@Fe_{0.1}$	Fe (0.1%)
$Y_{123}@Fe_{0.3}$	Fe (0.3%)
$Y_{123}@Fe_{0.5}$	Fe (0.5%)
$Y_{123}@Fe_{0.7}$	Fe (0.7%)
$Y_{123}@Fe_{1}$	Fe (1%)

2.2. Methods of Research and Analysis

X-ray phase analysis of the samples was performed on DRON-4 using CuK-a radiation in the range of 20 values of 20–90° with a typical scanning speed of 2° per minute. The X-ray detector in this instrument moves around the sample and measures the intensity of these peaks and their position (i.e., diffraction angle 20). The highest peak is defined as the 100% peak, and the intensity of all other peaks is measured as a percentage of the 100% peak. These peaks are characteristic of a particular crystal structure and compound and can be identified using the JCPDS database. The measurement error of the device is about 1–2%.

Sample morphology and local microstructure analysis were performed using a scanning electron microscope (SEM), including grain and particle size assessments. We used a Quanta 3D 2001 Dual, FEI instrument to examine the microstructure of our samples.

Quantum Design PPMS EverCool II equipment was used to measure the superconductivity of samples in the irreversible field cooling (FC) and zero field cooling (ZFC) operating modes in the low temperature region. Environmental controls for samples included fields up to $\pm 16 \times 10$ Oe and a temperature range of 1.9–400 K. Instrument measurement error was approximately 2–3%.

3. Results and Discussion

3.1. Pure (Undoped) Sample

According to the result of XRD analysis (Table 2), the phase composition of the undoped pure sample consists mainly of the superconducting phase $YBa_2Cu_3O_{7.03}$ (87.6 wt%), and a small inclusion of non-superconducting phase such as Y_2BaCuO_5 (5.3 wt%) and CuO (7.1 wt%).

As can be seen from the XRD result (Figure 3), we were able to obtain a high-quality superconducting phase Y_{123}, which corresponds to the theoretical standard phase $YBa_2Cu_3O_7$. As is known, deficiency or excess of oxygen greatly affects the superconducting properties of the material. The critical temperature of the sample is high and equal to 92.3 K.

Table 2. Results of XRD analysis.

No.	Phase Name	Content, wt%
1	$Yba_2Cu_3O_{7.03}$ (Y_{123})	87.6
2	Y_2BaCuO_5	5.3
3	CuO	7.1

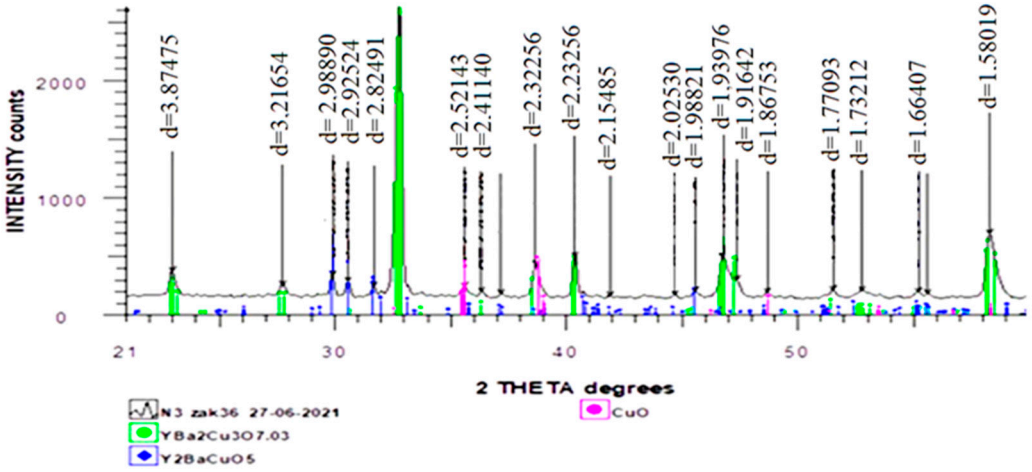

Figure 3. XRD analysis of a pure (undoped) sample.

On analyzing SEM images of the resulting sample, we saw the presence of many medium-sized grains and areas containing smaller, well-sintered grains (Figure 4). Thanks to the optimally selected force of pressing the initial mixtures into cylindrical shapes before initiating the combustion process, we obtained samples with the absence of any large micropores. As is known, dense samples without large micropores show the best results in terms of superconducting properties, in contrast to samples containing many micropores.

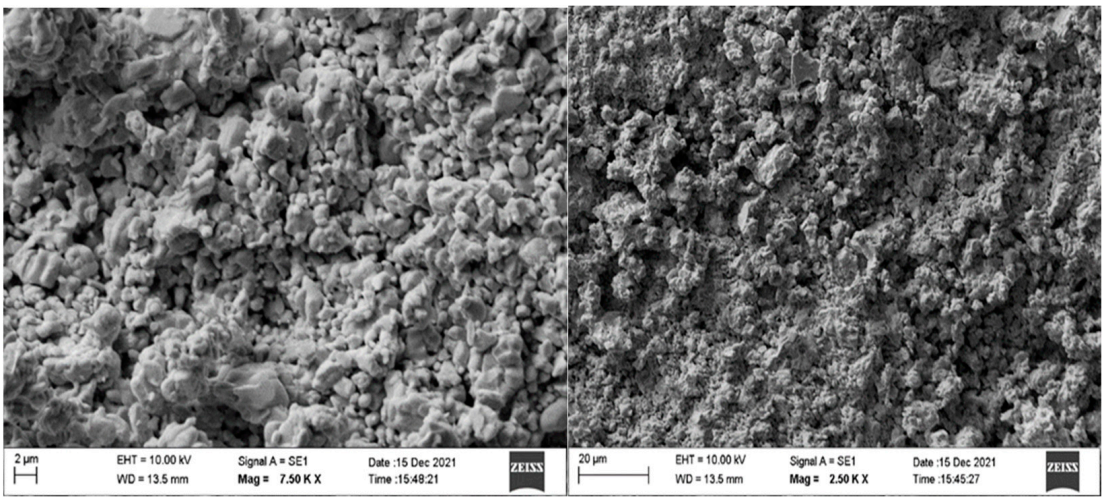

Figure 4. SEM micrographs of the surface of the sample $YBa_2Cu_3O_{7.03}$.

3.2. Samples Doped with Aluminum

Table 3 presents the XRD results of samples doped with aluminum microparticles from 0.1 wt% to 1.3 wt%. According to the analysis, the sample doped with aluminum at 1.0 wt% showed the highest yield in the formation of the superconducting phase, in contrast to others, and even higher than the pure undoped sample. When the percentage of doping with aluminum increased to 1.3 wt%, the formation of the superconducting

Y_{123} phase in the final composition sharply decreased. The critical temperature of the best sample, $Y_{123}@Al_1$, was 92.5 K, which was measured using a PPMS EVER Cool cryosystem; the rest had a slightly lower critical temperature value.

Table 3. Results of XRD analysis of samples doped with Al microparticles.

Phase Name	Content [wt%]					
	$Y_{123}@Al_{0.1}$	$Y_{123}@Al_{0.3}$	$Y_{123}@Al_{0.5}$	$Y_{123}@Al_{0.7}$	$Y_{123}@Al_1$	$Y_{123}@Al_{1.3}$
$YBa_2Cu_3O_{7.34}$	36.1	59.2	69.2	89.4	80.5	40.4
Y_2BaCuO_5	16.0	14.2	11.2	10.4	10.4	11.9
CuO	22.1	12.9	10.6	0.2	-	20.3
$BaCO_3$	14.6	2.5	1.2	-	-	15.7
$Y_2Cu_2O_5$	11.2	5.8	4.6	-	9.2	11.7

When doped with aluminum, a type of superconducting phase is formed as $YBa_2Cu_3O_{7.34}$, in contrast to the pure undoped $YBa_2Cu_3O_{7.03}$ sample. X-ray diffraction patterns of all samples are shown in Figure 5a–f.

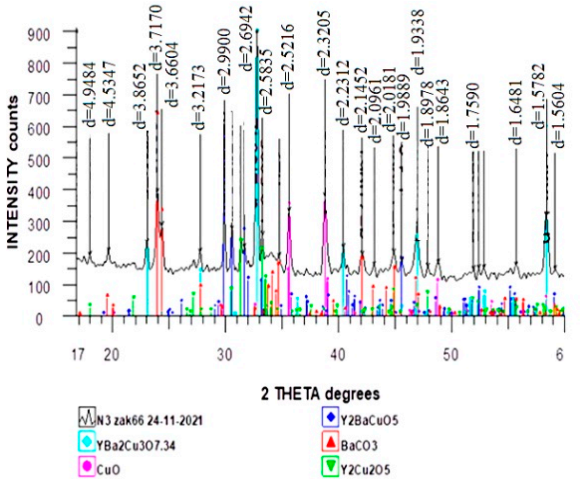

(**a**) Sample $Y_{123}@Al_{0.1}$.

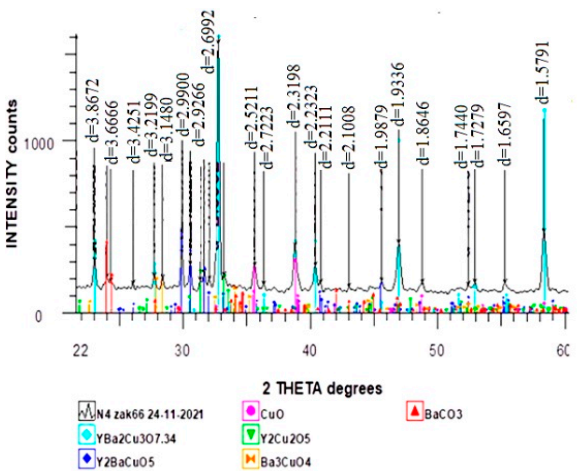

(**b**) Sample $Y_{123}@Al_{0.3}$.

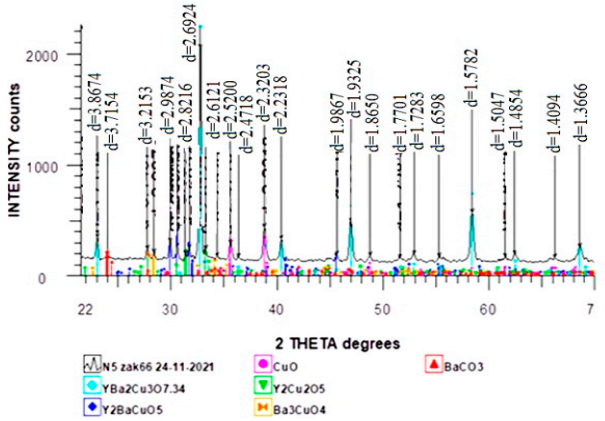

(**c**) Sample $Y_{123}@Al_{0.5}$.

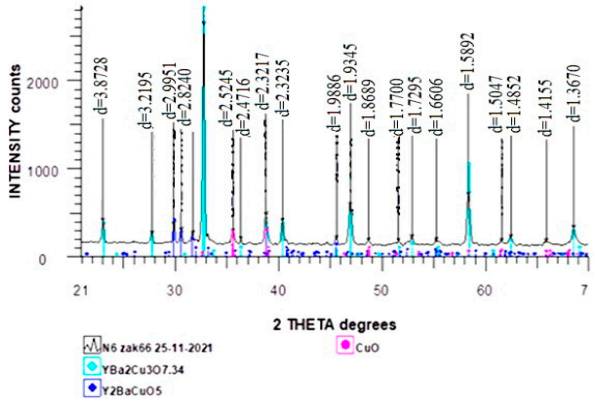

(**d**) Sample $Y_{123}@Al_{0.7}$.

Figure 5. *Cont*.

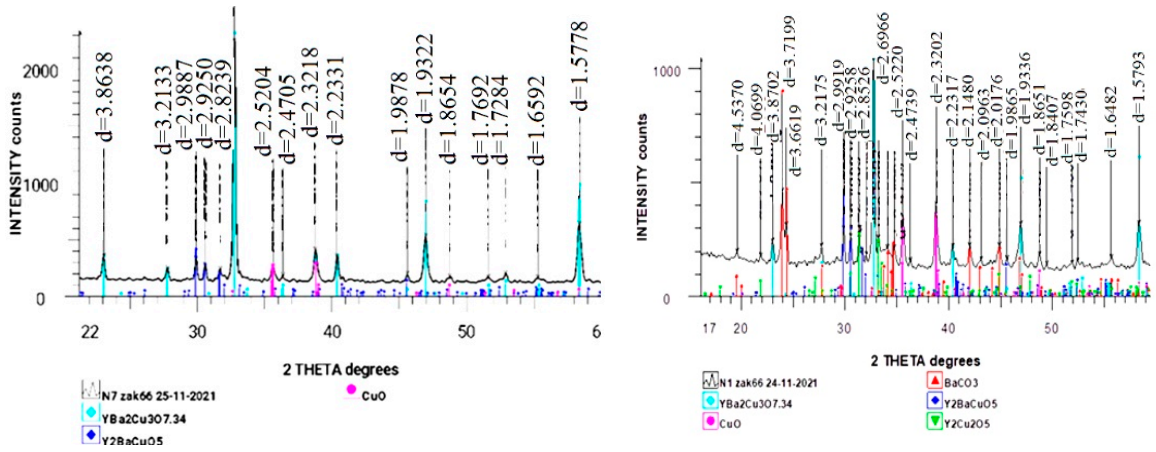

(**e**) Sample $Y_{123}@Al_{1.0}$ (**f**) Sample $Y_{123}@Al_{1.3.}$

Figure 5. X-ray diffraction patterns of samples doped with Al microparticles.

The microstructure of the samples was studied using scanning electron microscopy (SEM). The results of this study are presented in Figure 6a,b.

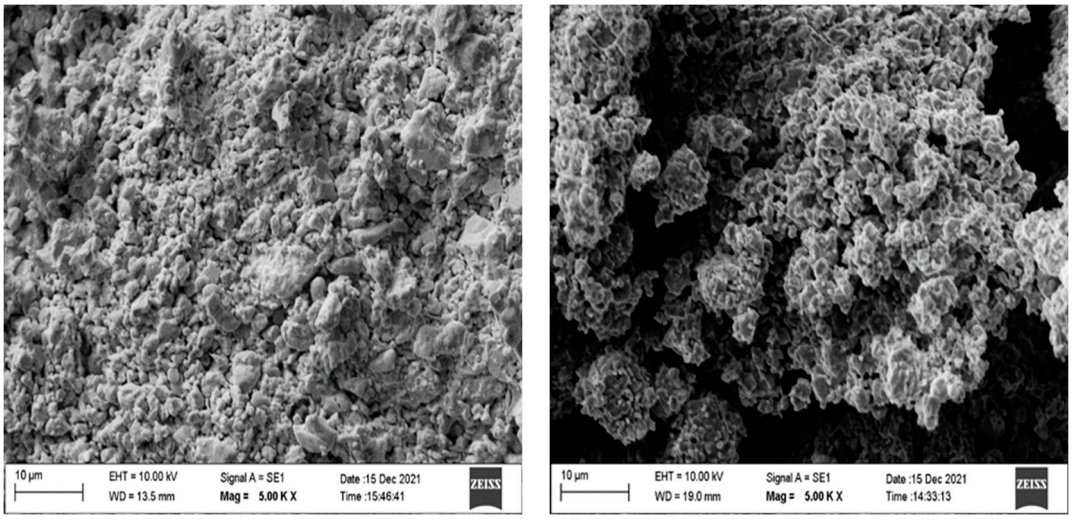

(**a**) Sample $Y_{123}@Al_{0.7}$ (**b**) Sample $Y_{123}@Al_{1.3}$

Figure 6. SEM micrographs of the sample surface $Y_{123}@Al_1$ and $Y_{123}@Al_{1.3}$.

The micrographs show characteristic changes in the microstructure, caused by the percentage of doping. When the content of aluminum microparticles is higher than 1.3 wt%, the sample has many microcavities, in contrast to the sample doped with 0.7 wt% aluminum. This is apparently due to the formation of a large amount of barium carbonate and copper oxide. It should be noted that aluminum does not form a separate phase, but is part of the superconducting phase, which is evidenced by an increase in grain sizes. The grain sizes of the aluminum-doped samples are in the range of 16–19 µm, which is slightly larger than the grain size in pure samples (13–15 µm).

The thermal analysis results (TG–DTA) for a pure and aluminum-doped sample are displayed in Figure 7.

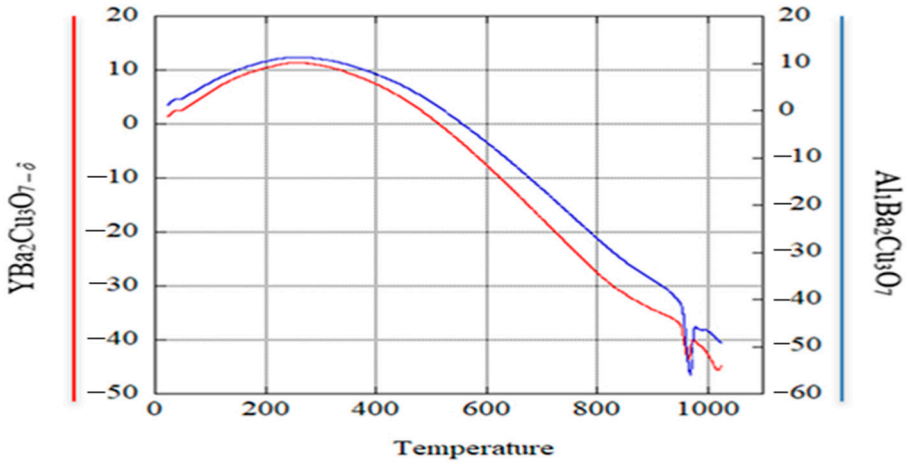

Figure 7. TG/DTA for pure sample and Y_{123}@$Al_{0.7}$.

TG-DTA results provide information about the thermal properties of the sample. Thermal analysis involves measuring changes in mass (TG) and thermal effects (DTA) of a sample as temperature changes. The TG-DTA results can help determine what changes occur in the structure and the thermal properties of a material when doped with Al. The results of TG-DTA analysis showed the following features:

- Mass changes (TG): There was some decrease in sample mass with increasing temperature. This may be due to the processes of desorption or decomposition of some components in the YBCO structure.
- Differential thermal analysis (DTA): During the heating of the sample, peaks of 920–960 °C of endothermic reactions were detected. This may indicate phase transitions or chemical reactions occurring in the material.
- Changes with doping: Comparison of results with undoped and aluminum doped YBCO samples showed significant differences in the TG-DTA curves. This confirms that aluminum doping affects the thermal behavior of the material due to its good reactivity. Consequently, it might be able to speed up the chemical reaction of the whole mixture. Pure samples have higher energy activation values than aluminum doped samples. This means that pure samples require much more energy to initiate a chemical reaction process.

3.3. Samples Doped with Iron Microparticles

Table 4 presents the results of XRD of samples doped with iron microparticles from 0.1 wt% to 1.0 wt%. According to the analysis (Figure 8), the sample doped with iron at 0.3 wt% showed the greatest formation of superconducting phase, unlike the others. When the percentage of iron doping increases to 1.0 wt%, there is a sharp decrease in the formation of the superconducting Y_{123} phase in the composition. As with samples doped with aluminum microparticles ($YBa_2Cu_3O_{7.34}$), when doped with iron microparticles, a superconducting phase ($YBa_2Cu_3O_{7.34}$) is formed with a slight excess of oxygen from the theoretical standard stoichiometric phase ($YBa_2Cu_3O_7$). Apparently microparticles of iron and aluminum promote the formation of a superconducting phase with a slight excess of oxygen during solid-phase combustion. The results also showed the absence of a $BaCO_3$ crystalline phase, which is positive since $BaCO_3$ is not a desirable component in the YBCO superconductor structure. The critical temperature of the best sample Y_{123}@$Fe_{0.3}$ was 92.1 K, which was measured using a PPMS EVER Cool cryosystem.

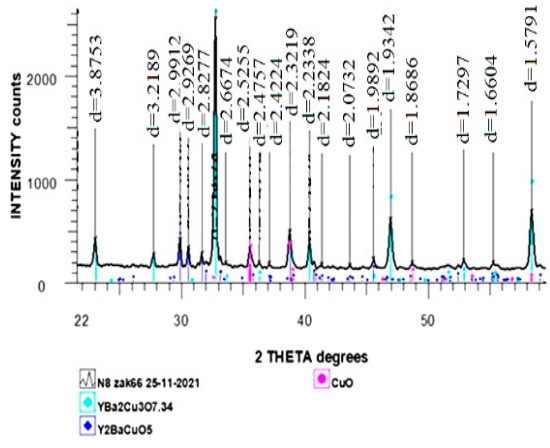

(**a**) Sample Y_{123}@Fe $_{0.1}$.

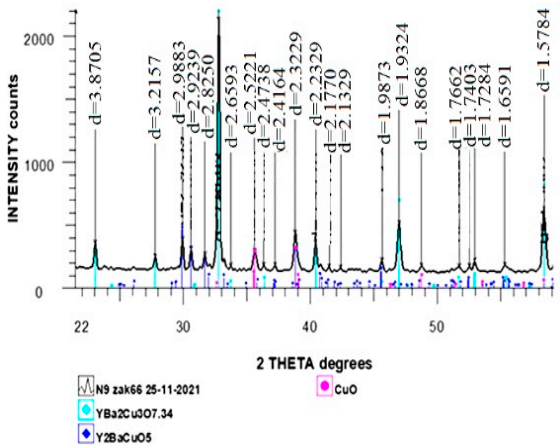

(**b**) Sample Y_{123}@Fe$_{0.3}$.

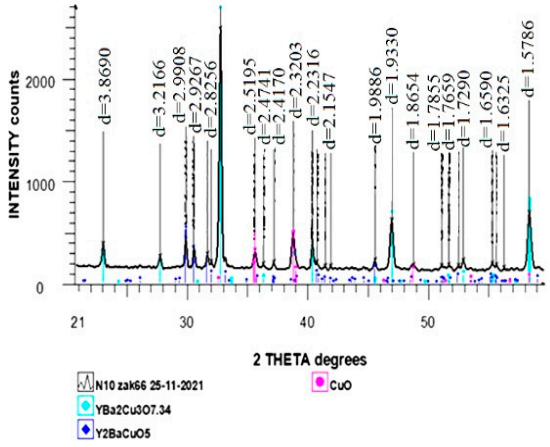

(**c**) Sample Y_{123}@Fe $_{0.5}$.

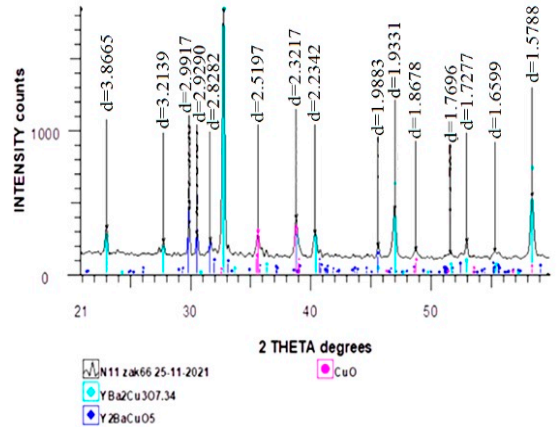

(**d**) Sample Y_{123}@Fe $_{0.7}$.

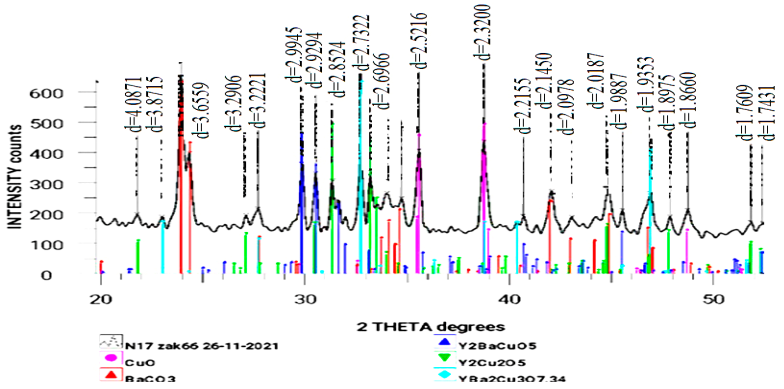

(**e**) Sample Y_{123}@Fe$_{1.0}$

Figure 8. X-ray diffraction patterns of samples doped with Fe microparticles.

X-ray diffraction patterns of all samples are shown in Figure 8a–e.

The micrographs (Figure 9) show characteristic changes in the microstructure due to the percentage of doping. The sample has a fine-grained structure and contains a small number of micropores. Apparently, as in the case of samples doped with aluminum, a large amount of copper oxide leads to the appearance of such small micropores.

Table 4. Results of XRD analysis of Fe-doped samples.

Phase Name	Content [wt%]				
	$Y_{123}@Fe_{0.1}$	$Y_{123}@Fe_{0.3}$	$Y_{123}@Fe_{0.5}$	$Y_{123}@Fe_{0.7}$	$Y_{123}@Fe_{1}$
$YBa_2Cu_3O_{7.34}$	72.3	75.2	60.0	24.8	12.4
Y_2BaCuO_5	15.3	14.1	18.8	29.8	21.9
CuO	12.4	10.7	16.4	24.9	24.5

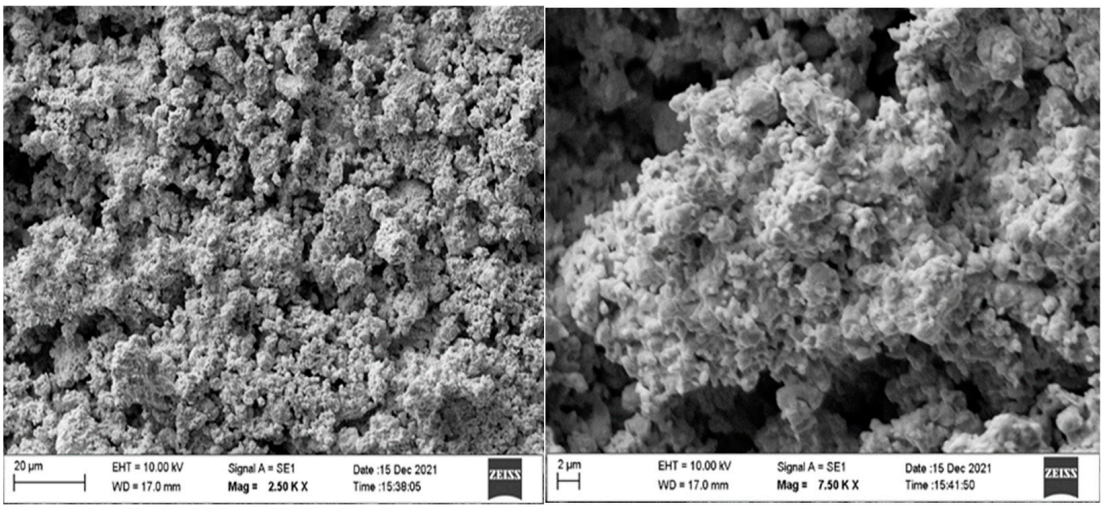

Figure 9. SEM micrographs of the surface of samples doped with Fe.

A temperature peak in the range of 920–960 °C indicates the presence of a phase transition or thermal event that occurs in this temperature range. This may be due to changes in the structure or composition of the material (Figure 10). Net mass losses that are greater than those resulting from iron doping may indicate that the addition of iron to the material affects its thermal behavior. This may be due to the formation of new phases or chemical reactions that change the decomposition process of the material when it is heated.

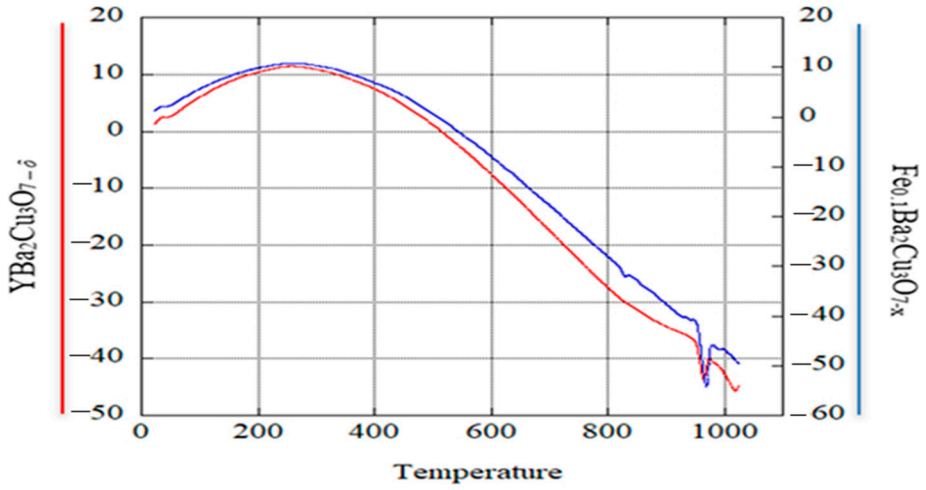

Figure 10. TG/DTA for pure sample and $Y_{123}@Fe_{0.1}$.

3.4. Samples Doped with Nickel

Table 5 presents the results of X-ray diffraction of samples doped with nickel microparticles from 0.1 wt% to 1.0 wt%. According to the analysis (Figure 11), the sample doped with nickel at 0.5 wt% showed the greatest formation of superconducting phase, unlike the

others. With an increase in the percentage of nickel doping to 1.0 wt%, there is a decrease in the formation of the superconducting Y_{123} phase in the composition. When doped with nickel microparticles, like iron and aluminum, a superconducting phase ($YBa_2Cu_3O_{7.34}$) is formed with a slight excess of oxygen from the theoretical standard stoichiometric phase ($YBa_2Cu_3O_7$). Apparently nickel also enriches the main phase with oxygen during solid-phase combustion. The results also showed the absence of the $BaCO_3$ crystalline phase (except at a doping level of 1.0 wt%) which is a positive point. It should also be noted that the non-superconducting phase Y_2BaCuO_5 begins to increase in composition with increasing percentage of nickel doping, reaching 18.7 wt%. The critical temperature of the best sample $Y_{123}@Ni_{0.5}$ is 92.2 K, which was measured using a PPMS EVER Cool cryosystem.

Table 5. Results of XRD analysis of samples doped with Ni microparticles.

Phase Name	Content [wt%]				
	$Y_{123}@Ni_{0.1}$	$Y_{123}@Ni_{0.3}$	$Y_{123}@Ni_{0.5}$	$Y_{123}@Ni_{0.7}$	$Y_{123}@Ni_1$
$YBa_2Cu_3O_{7.34}$	74.0	72.2	74.7	68.3	65.9
Y_2BaCuO_5	14.5	17.1	14.8	18.7	17.8
CuO	11.5	10.7	10.6	13.0	14.2
$BaCO_3$	-	-	-	-	2.1

X-ray diffraction patterns of samples doped with Ni microparticles are presented in Figure 11a–e.

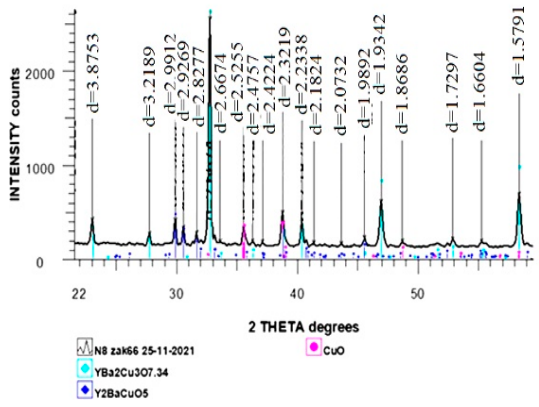

(**a**) Sample $Y_{123}@Ni_{0.1}$.

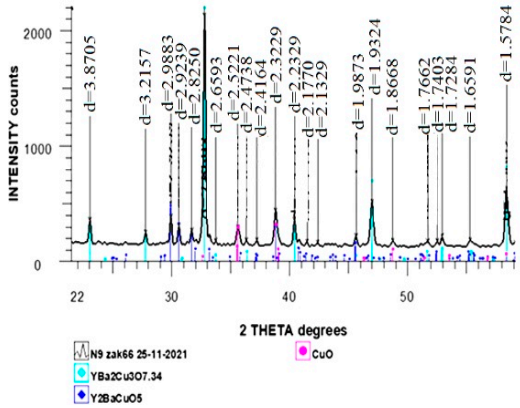

(**b**) Sample $Y_{123}@Ni_{0.3}$.

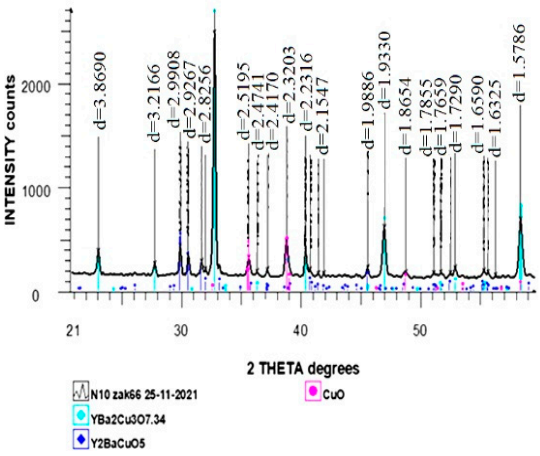

(**c**) Sample $Y_{123}@Ni_{0.5}$.

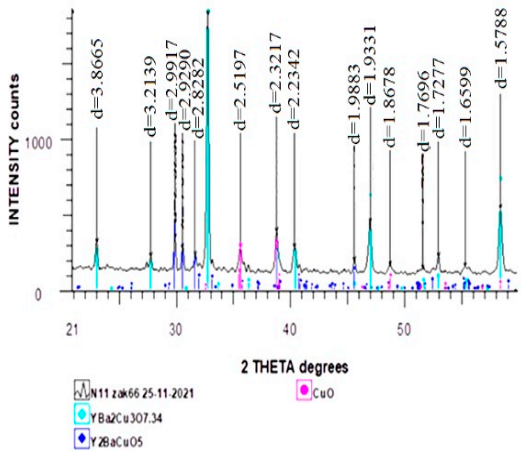

(**d**) Sample $Y_{123}@Ni_{0.7}$.

Figure 11. *Cont.*

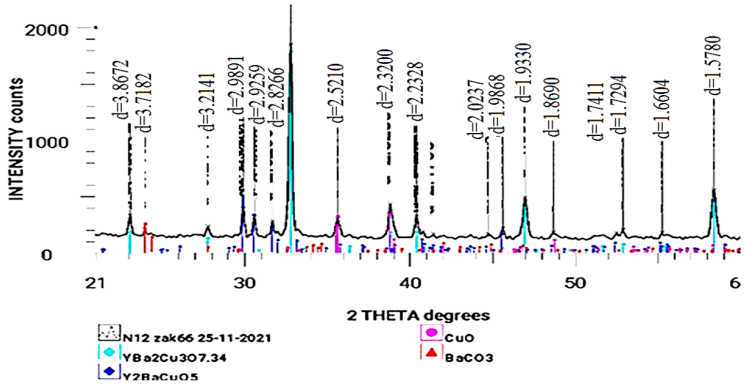

(**e**) Sample $Y_{123}@Ni_{1.0}$

Figure 11. X-ray patterns of samples doped with nickel.

Figure 12 shows that the image has a fine-grained structure; the particle (grain) sizes are in the range of 3–6 microns. There is also a small inclusion of micropores.

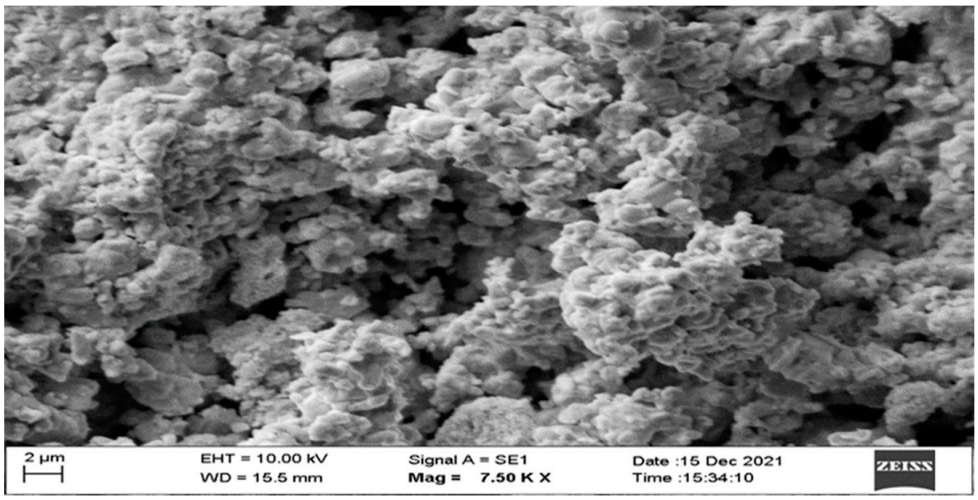

Figure 12. Micrograph of a sample doped with nickel.

The results of thermal analysis (TG–DTA), pure sample and doped Ni sample, are presented in Figure 13.

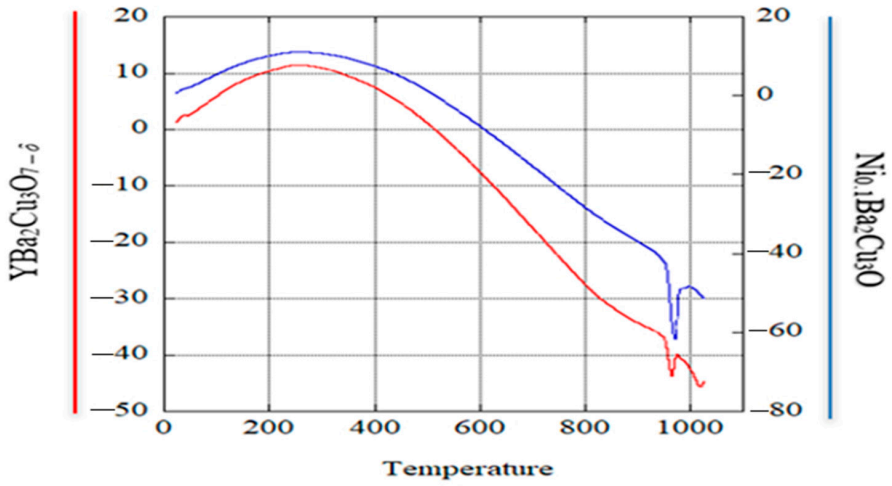

Figure 13. TG/DTA for pure sample and $Ni_{0.1}Ba_2Cu_3O_{7-x}$.

The doped sample with the addition of 0.1 percent nickel microparticles has less mass loss compared to the pure sample. The mass loss is −75 mg in the pure sample and −50 mg in the doped sample, indicating that the addition of nickel may influence the thermal behavior of the material.

4. Conclusions

YBCO-based superconducting composites doped with microparticles were synthesized. By including the process of preliminary mechanical activation of the starting components (before solid-phase combustion), the total time of heat treatment and thereby the procurement of the final material was reduced significantly. It has been established that the percentage of doping with modifying additives, heat treatment, and holding time directly affect the qualitative and quantitative formation of the useful superconducting phase Y_{123}, which in turn affects the basic superconducting properties of the final material.

X-ray diffraction analysis showed that the sample in its pure form is an almost ideal stoichiometric superconducting phase ($YBa_2Cu_3O_{7.03}$), and in samples doped with microparticles of iron, aluminum, and nickel the superconducting phase has a different form ($YBa_2Cu_3O_{7.34}$) with a slight increase in the oxygen index in the formed phase.

It should be noted that the method of solid-phase combustion produces high-quality samples both in the pure form and when doped with microparticles. All samples have approximately the same critical temperature. It is important to point out that when doped with aluminum microparticles (Y_{123}@$Al_{0.7}$), the critical temperature is higher than that of a pure sample, and the yield of the superconducting phase is higher than that of all others, including the synthesis of a pure sample. Based on this, it should be noted that aluminum microparticles could be used as a modifying additive to obtain various types of superconducting composite of the YBCO for practical applications.

Author Contributions: Conceptualization, S.T.; methodology, S.T.; investigation, A.S.; writing—original draft preparation, S.T. and A.S.; writing—review and editing, S.T. and S.F. All authors have read and agreed to the published version of the manuscript.

Funding: This research was funded by the Science Committee of The Ministry of Science and Higher Education of the Republic of Kazakhstan (Grant No. AP19677755).

Data Availability Statement: All data will be provided by requesting via the corresponding email.

Conflicts of Interest: The authors declare no conflict of interest.

References

1. Antipov, E.V.; Abakumov, A.M. Structural design of superconductors based on complex copper oxides. *UFN* **2008**, *178*, 190–202.
2. Blatter, G.; Fogelman, M.V.; Geshkenbein, V.B. Vortices in high temperature superconductors. *Rev. Mod. Phys.* **1994**, *66*, 1125–1380. [CrossRef]
3. MacManus-Driscoll, J.; Wimbush, S. Future Directions for Cuprate Conductors. *IEEE Trans Appl. Supercond.* **2011**, *21*, 2495–2500. [CrossRef]
4. Sahoo, B.; Routray, K.L.; Mirdha, G.C.; Karmakar, S.; Singh, A.K.; Samal, D.; Behera, D. Investigation of microhardness and superconducting parameters of CNTs blended YBCO superconductor. *Ceram Int.* **2019**, *45*, 22055–22066. [CrossRef]
5. Hamideh, S.; Hosseini, S.S.; Ghotb, S.S.; Sichani, B.H.; Sepideh, P. Magnetic doping effects on the superconductivity of Y1-xMx$Ba_2Cu_3O_{7-\delta}$ (M = Fe Co, Ni). *Ceram Int.* **2021**, *47*, 10635–10642.
6. Alotaibi, S.A.; Slimani, Y.; Hannachi, E.; Almessiere, M.E.; Yasin, G.; Al-Qwairi, F.O.; Iqbal, M.; Ben Azzouz, F. Intergranular properties of polycrystalline $YBa_2Cu_3O_{7-\delta}$ superconductor added with nanoparticles of WO_3 and $BaTiO_3$ as artificial pinning centers. *Ceram Int.* **2021**, *47*, 34260–34268. [CrossRef]
7. Huhtinen, H.; Awana, V.P.; Gupta, A.; Kishan, H.; Laiho, R.; Narlikar, A.V. Pinning centers and enhancement of critical current density in YBCO doped with Pr, Ca, and Ni. *Supercond. Sci. Technol.* **2007**, *20*, 159–166. [CrossRef]
8. Volokhova, D.; Piovarchi, S.; Hospodowska, M.; Antal, V.; Kovacs, J.; Jurek, K.; Yirsa, M.; Diko, P. YBCO bulk superconductors doped with gadolinium and samarium. *Phys. C Supercond.* **2013**, *494*, 36–40. [CrossRef]
9. Tolendiuly, S.; Alipbayev, K.; Fomenko, S.; Sovet, A.; Zhauyt, A. Properties of high-temperature superconductors (HTS) and synthesis technology. *Metalurgija* **2021**, *60*, 137–140.
10. Rao, C.N.R.; Nagarajan, R.; Vijayaraghavan, R. Synthesis of Cuprate Superconductors. *Supercond. Sci. Technol.* **1993**, *6*, 1. [CrossRef]

11. Zhang, Y.; Yang, H.; Li, M.; Sun, B.; Qi, Y.; Zhang, Y.; Yang, H.; Li, M.; Sun, B.; Qi, Y. Improvement of multiple oxide properties: Effect of gel processes on the quality of $Bi_2Sr_2CaCu_2O_{8+\delta}$ superconducting powders. *Cryst. Eng. Comm.* **2010**, *12*, 3046. [CrossRef]
12. Keyson, D.; Longo, E.; Vasconcelos, J.S.; Varela, J.A.; Éber, S.; Der Maderosian, A. Synthesis, and ceramics processing by domestic microwave oven. *Cerâmica* **2006**, *52*, 50–56. [CrossRef]
13. Tolendiuly, S.; Fomenko, S.M.; Abdulkarimova, R.G.; Akishev, A. Synthesis and superconducting properties of the MgB_2@BaO composites. *Inorg. Nano-Met. Chem.* **2020**, *50*, 349–353. [CrossRef]